REPORT DOCUMENTATION PAGE	*Form Approved* *OMB No. 0704-0188*

Public reporting burden for this collection of information is estimated to average 1 hour per response, including the time for reviewing instructions, searching existing data sources, gathering and maintaining the data needed, and completing and reviewing the collection of information. Send comments regarding this burden estimate or any other aspect of this collection of information, including suggestions for reducing this burden, to Washington Headquarters Services, Directorate for Information Operations and Reports, 1215 Jefferson Davis Highway, Suite 1204, Arlington, VA 22202-4302, and to the Office of Management and Budget, Paperwork Reduction Project (0704-0188), Washington, DC 20503.

1. AGENCY USE ONLY *(Leave blank)*

2. REPORT DATE
September 1992

3. REPORT TYPE AND DATES COVERED
Technical Paper

4. TITLE AND SUBTITLE
A Method for Designing Blended Wing-Body Configurations for Low Wave Drag

5. FUNDING NUMBERS
WU 505-59-53-01

6. AUTHOR(S)
Raymond L. Barger

7. PERFORMING ORGANIZATION NAME(S) AND ADDRESS(ES)
NASA Langley Research Center
Hampton, VA 23681-0001

8. PERFORMING ORGANIZATION REPORT NUMBER
L-17095

9. SPONSORING/MONITORING AGENCY NAME(S) AND ADDRESS(ES)
National Aeronautics and Space Administration
Washington, DC 20546-0001

10. SPONSORING/MONITORING AGENCY REPORT NUMBER
NASA TP-3261

11. SUPPLEMENTARY NOTES

12a. DISTRIBUTION/AVAILABILITY STATEMENT

Unclassified–Unlimited

Subject Category 02

12b. DISTRIBUTION CODE

13. ABSTRACT *(Maximum 200 words)*
A procedure for tailoring a blended wing-body configuration to reduce its computed wave drag is described. The method utilizes an iterative algorithm within the framework of first-order linear theory. Four computed examples are included. In each case, the zero-lift wave drag was reduced without an increase in drag due to lift.

14. SUBJECT TERMS
Supersonic aircraft design; Blended wing-body; Low-drag design

15. NUMBER OF PAGES
17

16. PRICE CODE
A03

17. SECURITY CLASSIFICATION OF REPORT	18. SECURITY CLASSIFICATION OF THIS PAGE	19. SECURITY CLASSIFICATION OF ABSTRACT	20. LIMITATION OF ABSTRACT
Unclassified	Unclassified		

Abstract

A procedure for tailoring a blended wing-body configuration to reduce its computed wave drag is described. The method utilizes an iterative algorithm within the framework of first-order linear theory. Four computed examples are included. In each case, the zero-lift wave drag was reduced without an increase in drag due to lift.

Introduction

In the initial rough-cut state of supersonic configuration design, the requirement for low wave drag is a prime consideration. Often, at this stage in the design process, linear codes are used to compute the lift and the drag due to lift (ref. 1) as well as the zero-lift drag (ref. 2).

Reference 2 includes a design option for tailoring the fuselage of a configuration to obtain low zero-lift wave drag. However, this procedure has several weaknesses. It is applicable only if the configuration has a fuselage that is defined by circular cross sections. The procedure is based on the zero-order-accuracy Eminton-Lord theory (ref. 3), by which the computed drag is independent of Mach number. This independence is inconsistent with the first-order theory (ref. 4) that is used in the analysis phase of the program to compute drag from the equivalent area distributions obtained from Mach plane slices. Finally, the procedure does not account for the volume that is required to fill the gap that occurs between the fuselage and the wing when these two components are input separately in the wave-drag geometry format.

This paper describes a method for tailoring a blended wing-body configuration for low wave drag. The method utilizes Mach plane slice area distributions and so is consistent with the wave-drag analysis. Furthermore, since for a blended wing-body the fuselage geometry is not input as a separate component to the wave-drag program, there is no requirement to account for the fuselage-wing gap. The method designs for low drag at zero lift in accordance with the first-order analysis procedures of reference 2, and then the methods of reference 1 are used to ensure that this tailoring does not increase the drag at the design lift coefficient.

Symbols

B	base area of body of revolution
B_b	equivalent base area corresponding to displacement effect of jet exhaust
$C_{D,wl}$	drag coefficient due to lift at design lift coefficient
C_L	lift coefficient
$C_{D,w0}$	zero-lift drag coefficient
D_w	zero-lift wave drag
$E(x)$	error distribution
L	length of equivalent body
M	Mach number
MSAD	Mach slice area distribution
q	dynamic pressure
S	synthesized distribution obtained by averaging individual equivalent area distributions
S_r	cross-sectional area of body of revolution
S_θ	equivalent area—area of Mach plane slice at polar angle θ through configuration, projected onto YZ-plane
T	thickness along centerline section
V	volume; volume parameter
X	$= x/L$
x, y, z	Cartesian coordinates
$\Delta D_{w,i}$	wave-drag component corresponding to θ_i set of Mach plane slices
η, ξ	dummy integration variables
θ	angle between Y-axis and projection of Mach plane slice normal vector onto YZ-plane

Analysis

Linear Wave-Drag Equations

Reference 4 shows that the linear theory approximation to the wave drag of a general, slender, nonlifting configuration is

$$D_w = \int_0^{2\pi} \frac{dD_w}{d\theta}\, d\theta \tag{1}$$

where $\frac{dD_w}{d\theta}$ is the wave drag associated with the θ set of Mach plane slices. These are the Mach planes whose surface normal vectors project onto the YZ-plane at angle θ to the Y-axis. (See fig. 1.)

Equation (1) is approximated by the sum of a finite number of Mach slice drag components:

$$D_w \approx \frac{1}{n} \sum_{i=1}^{n} \Delta D_{w,i} \tag{2}$$

The increments $\Delta D_{w,i}$ are defined by the formula

$$\Delta D_{w,i} = -\frac{q}{2\pi} \int_0^L \int_0^L \left[S''_{\theta i}(\xi)\, S''_{\theta i}(\eta) \ln|\xi - \eta| \; d\xi \; d\eta \right] \tag{3}$$

where $S_{\theta i}$ is the equivalent area associated with the Mach plane slices at angle θ_i. The primes indicate differentiation with respect to x. The equivalent area is the area of the projection of the Mach plane slice through the body onto the YZ-plane (fig. 1).

The Design Problem

The design problem for low wave drag is to find a feasible configuration geometry for which the second derivative distributions in equation (3) yield a low value of D_w in equation (2). It may be instructive to compare this problem with the design problem for low sonic boom (ref. 5), which specifies a target equivalent area distribution for only one set of Mach slices (that at $\theta = -90°$). With the planform and the camber distribution considered to be fixed, a straightforward iterative procedure can be used to tailor the thickness distribution to obtain the required equivalent area distribution (ref. 6). In contrast, the wave-drag design problem involves multiple equivalent area distributions. Tailoring the thickness distributions for any one of these could have a negative impact on the other distributions. This effect was demonstrated in an initial abortive attempt at synthesizing a design procedure. For this attempt, 16 Mach plane sliced area distributions were used. Because of symmetry only nine distributions needed to be calculated. Each distribution was written out, together with the wave drag associated with that distribution. The distribution associated with the largest value of wave drag was then subjected to a smoothing procedure to generate a highly smoothed version of the original distribution. The smoothed distribution was then used as the target distribution for tailoring the thicknesses of the wing-fuselage sections to reduce the wave drag for this particular Mach slice distribution. This procedure always reduced the wave drag for that distribution and, to a lesser extent, it usually reduced the wave drag associated with the adjacent distributions. For the remaining distributions the drag increments varied between positive and negative so that the total drag increment was sometimes a net increase. This method succeeded in reducing the drag only for poor initial designs (those having very high drag); consequently, it was rejected.

Detailed Procedure

The method that was adopted utilizes a more global approach. The procedure is described here, and a flow diagram is given in figure 2.

First, the individual equivalent area distributions are computed and averaged. The result is a single synthesized distribution having a value of zero at the nose ($x = 0$) and terminating in a value B_b, which is the equivalent area associated with the displacement effect associated with the jet plume and the wake.

Next, this synthesized distribution is compared with the minimum drag area distribution for a body of revolution having a positive base area $B = B_b$ (ref. 7):

$$S_r(x) = \frac{8}{3} \frac{V - B}{\pi} \left(1 - X^2\right)^{3/2} + \frac{B}{\pi} X \sqrt{1 - X^2} + \frac{B}{\pi} \cos^{-1} X \tag{4}$$

where V is the volume of the body of revolution; but when equation (4) is used as a target distribution for an aircraft geometry, V is treated as a design parameter that controls the configuration volume, which is generally slightly less than V. An option in the computer code described in reference 2 permits one to compute the actual overall volume of a configuration. The value of V to be used in equation (4) to obtain the required configuration volume is ultimately determined by iteration.

The third step in the procedure is to alter the thickness distribution of the wing-body along Mach cone slices. Thus, for each value of x for which the synthesized distribution is computed, a double Mach cone is constructed with its axis aligned with the flight direction axis and its vertex at the given value of x. For this x, the synthesized distribution is compared with the target distribution. If the synthesized distribution is larger, the thicknesses are reduced proportionately where the Mach cone intersects the wing-body. Similarly they are increased where the synthesized distribution underestimates the target distribution. These thickness variations can be applied along the forward part of the Mach cone, the rearward part, or both.

This process is iterated until an approximation to the target distribution is obtained. The target distribution will not be obtained precisely because the thickness changes are applied vertically (in the z-direction) and not in the Mach slice direction. Consequently, attempts to refine a design beyond a reasonable point tend to cause "wiggles" in the distribution area. These wiggles result in large values in the second derivatives in equation (4) and thereby increase the drag. Only three or four iterations are required to obtain a smooth approximation to the target distribution (fig. 3). One determines the actual number of iterations required by examining the drag computed by equation (2) in each analysis iteration, stopping the iteration when it begins to increase, and backing up one iteration.

The final step in the procedure is to satisfy the volume constraint. The volume of the redesigned configuration is compared with the required volume, and the value of V in equation (4) is altered proportionately. Then the entire procedure is repeated to obtain the required volume within a specified error bound.

We evaluate the design by comparing the zero-lift wave drag of the configuration with that of the original configuration using 64 Mach slice distributions in the analysis. Also, the induced drag due to lift at the required lift coefficient is compared with that of the original configuration.

There is little mathematical basis for the above procedure. If the drag increment computed by equation (3) were a linear functional of the corresponding area distributions, then the synthesized average area distribution could be used to compute an average drag. As it is, this average area distribution cannot be used to compute any meaningful drag value except for a body of revolution.

Intuitively, however, the procedure *does* provide a means of obtaining a kind of global improvement in the volume distribution so that the sum of the individual drag increments is decreased. The procedure has succeeded in reducing the computed wave drag for all cases attempted thus far, even when considerable effort has been expended to generate a low-drag initial configuration. Several of these sample cases are described in the following section.

Sample Cases

The following examples were generated strictly for the purpose of illustrating the effectiveness of the procedure for reducing the wave drag. No attempt was made to satisfy the many constraints associated with factors such as engine sizing or distribution of weight and volume that would be required for a practical configuration designed for a specific mission. On the other hand, some effort was made to generate initial configurations with relatively low wave drag, so that a further reduction of the drag would be a significant accomplishment. Although the thickness was tailored to reduce the drag, the planform was not changed, and the overall volume, the lift, and the base area associated with the jet exhaust were held essentially constant. All the configurations included a vertical fin and four generic engine nacelles but no horizontal tail or canard (fig. 4(a)). For the second example, the fuselage cross-section shapes were nearly circular, but for the other cases, the fuselage cross sections were more nearly elliptical (fig. 4(b)).

Figure 5 shows the planform for the first example: a configuration designed for flight at $M = 1.6$. The overall planform area is 11 686 ft^2, the fuselage length is 295 ft, and the wing span is 155 ft. The wing leading edge is continuously curved, with a tip sweep angle of approximately 60°. The thickness distribution along the centerline is shown in figure 6, along with the revised thickness distribution. The results of the thickness tailoring are as follows:

Parameter	Initial	Revised
$C_{D,w0}$	0.00286	0.00132
$C_{D,wl}$	.00583	.00580
C_L	.10033	.10001
V, ft^3	40 467	40 395

The zero-lift wave drag is considerably reduced without significant variation in the other parameters.

Figure 7 shows the planform for the second example: a Mach 2.0 configuration. The planform area is 12 160 ft^2, the fuselage length is 295 ft, and the wing span is 156 ft. The leading edge has a straight segment having a sweep angle of 66°. The centerline thickness distributions are shown in figure 8, and the design results are as follows:

Parameter	Initial	Revised
$C_{D,w0}$	0.00269	0.00245
$C_{D,wl}$	.00733	.00712
C_L	.09831	.09816
V, ft^3	41 826	41 814

In this case, the reduction in $C_{D,w0}$ is only about 10 percent. This is augmented by a slight reduction in $C_{D,wl}$.

Figure 9 shows the planform for example 3, another Mach 2.0 configuration. The planform area is 11 975 ft^2, the fuselage length is 295 ft, and the wing span is 155 ft. The primary leading-edge sweep angle is 67°. The centerline thickness distributions are shown in figure 10, and the design results are as follows:

Parameter	Initial	Revised
$C_{D,w0}$	0.00236	0.00175
$C_{D,wl}$	.00667	.00644
C_L	.09945	.10005
V, ft^3	40 127	40 176

In this case a significant decrease in $C_{D,w0}$ is obtained, together with a slight decrease in $C_{D,wl}$.

The fourth example is a Mach 2.4 configuration whose planform is shown in figure 11. The planform area is 12 278 ft^2, the fuselage length is 295 ft, and the span is 151 ft. The primary leading-edge sweep angle is 69.1°. The centerline thickness distributions are shown in figure 12, and the design results are as follows:

Parameter	Initial	Revised
$C_{D,w0}$	0.00182	0.00154
$C_{D,wl}$	.00610	.00603
C_L	.08620	.08577
V, ft^3	40 212	40 235

Even though the $C_{D,w0}$ value for the original configuration is already quite low, it is further reduced in the design process.

For the sonic-boom-type designs (first, third, and fourth examples), a thinning occurs toward the aft portion of the section, but a compensating thickening occurs forward of this region, so that a nearly constant volume is maintained. This type of thickness redistribution occurs because of the far-aft maximum span position of the wing. This revised thickness distribution may pose additional structural and space-allocation problems. In the second example, however, which has the wing in a more forward location, the revision results in a more equitable thickness revision.

Concluding Remarks

A procedure for tailoring a blended wing-body configuration to reduce its wave drag has been described. The procedure utilizes an iterative loop within an analysis code that computes the zero-lift wave drag from multiple Mach plane slice area distributions. In the design process the geometry is constrained by holding essentially constant the planform shape, the overall volume, the lift, and the base area associated with the jet exhaust. Four sample cases were described. In each case the zero-lift wave drag was reduced without an increase in drag due to lift.

NASA Langley Research Center
Hampton, VA 23681-0001
August 3, 1992

References

1. Carlson, Harry W.; and Walkley, Kenneth B.: *Numerical Methods and a Computer Program for Subsonic and Supersonic Aerodynamic Design and Analysis of Wings With Attainable Thrust Considerations.* NASA CR-3808, 1984.

2. Middleton, W. D.; Lundry, J. L.; and Coleman, R. G.: *A System for Aerodynamic Design and Analysis of Supersonic Aircraft. Part 2—User's Manual.* NASA CR-3352, 1980.

3. Eminton, E.; and Lord, W. T.: Note on the Numerical Evaluation of the Wave Drag of Smooth Slender Bodies Using Optimum Area Distributions for Minimum Wave Drag. *J. Royal Aeronaut. Soc.*, vol. 60, no. 541, Jan. 1956, pp. 61–63.

4. Jones, Robert T.: *Theory of Wing-Body Drag at Supersonic Speeds.* NACA Rep. 1284, 1956. (Supersedes NACA RM A53H18a.)

5. Darden, Christine M.: *Sonic-Boom Minimization With Nose-Bluntness Relaxation.* NASA TP-1348, 1979.

6. Barger, Raymond L.; and Adams, Mary S.: *Fuselage Design for a Specified Mach-Sliced Area Distribution.* NASA TP-2975, 1990.

7. Adams, Mac C.: *Determination of Shapes of Boattail Bodies of Revolution for Minimum Wave Drag.* NACA TN 2550, 1951.

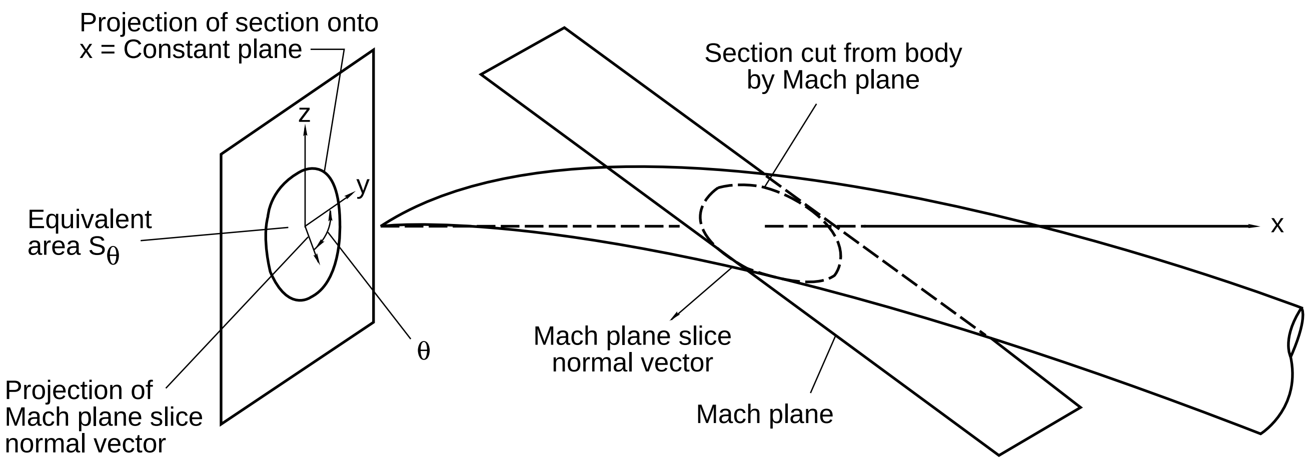

Figure 1. Geometric quantities for computing equivalent area.

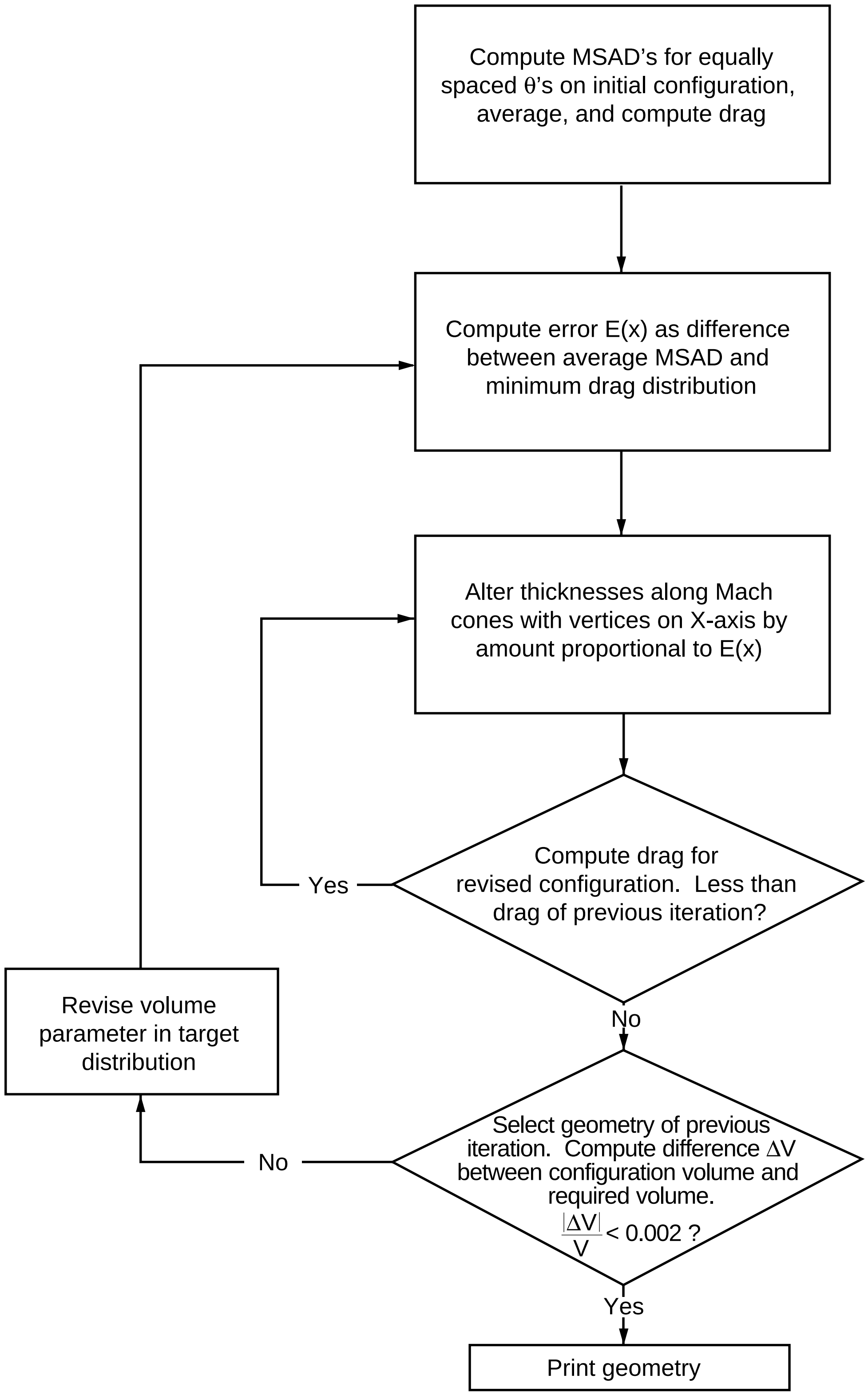

Figure 2. Flowchart of design procedure.

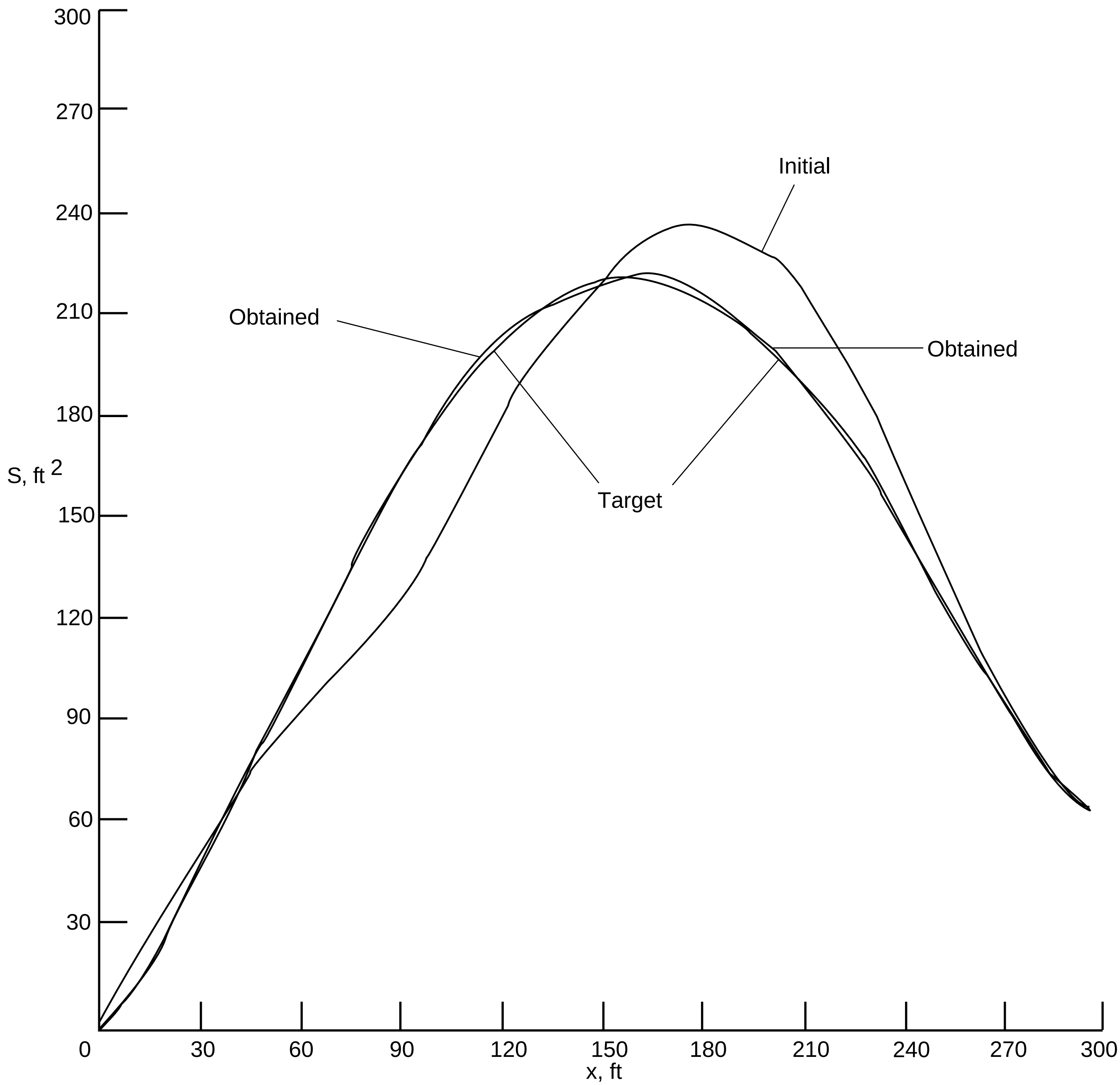

Figure 3. Sample calculation illustrating convergence capability of iterative procedure.

(a) General type of configuration considered.

(b) Typical cross-section shape.

Figure 4. Basic configuration geometry.

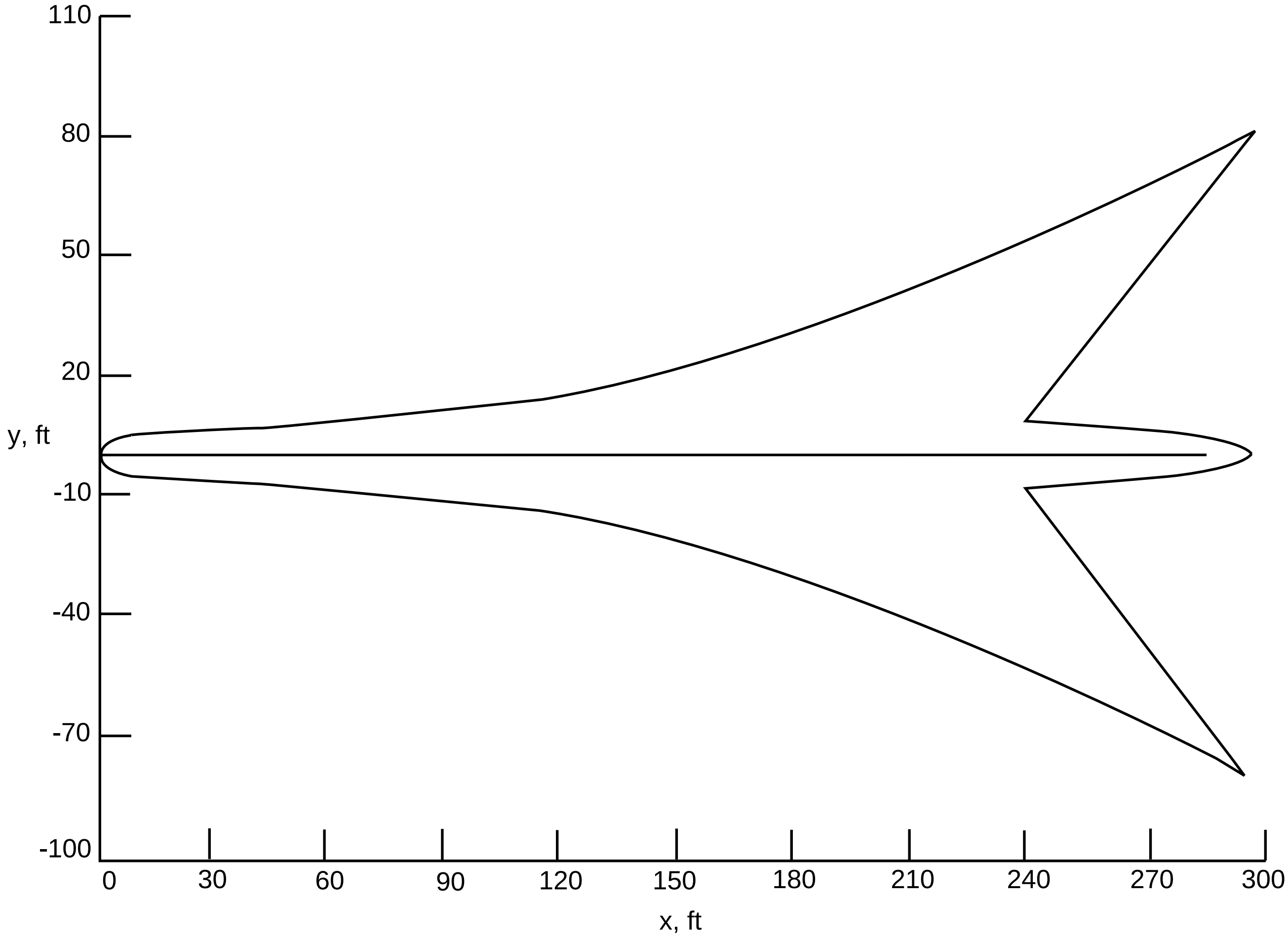

Figure 5. Planform of Mach 1.6 configuration.

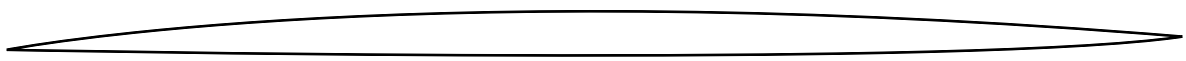

(a) Initial.

(b) Revised.

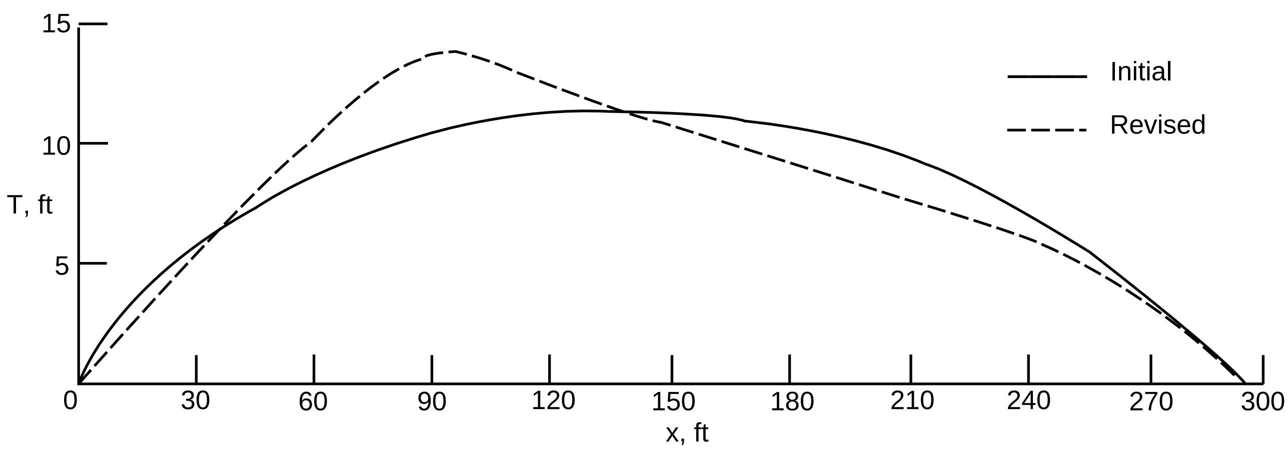

(c) Comparison of centerline thickness distributions.

Figure 6. Thickness distributions along centerline for Mach 1.6 configuration.

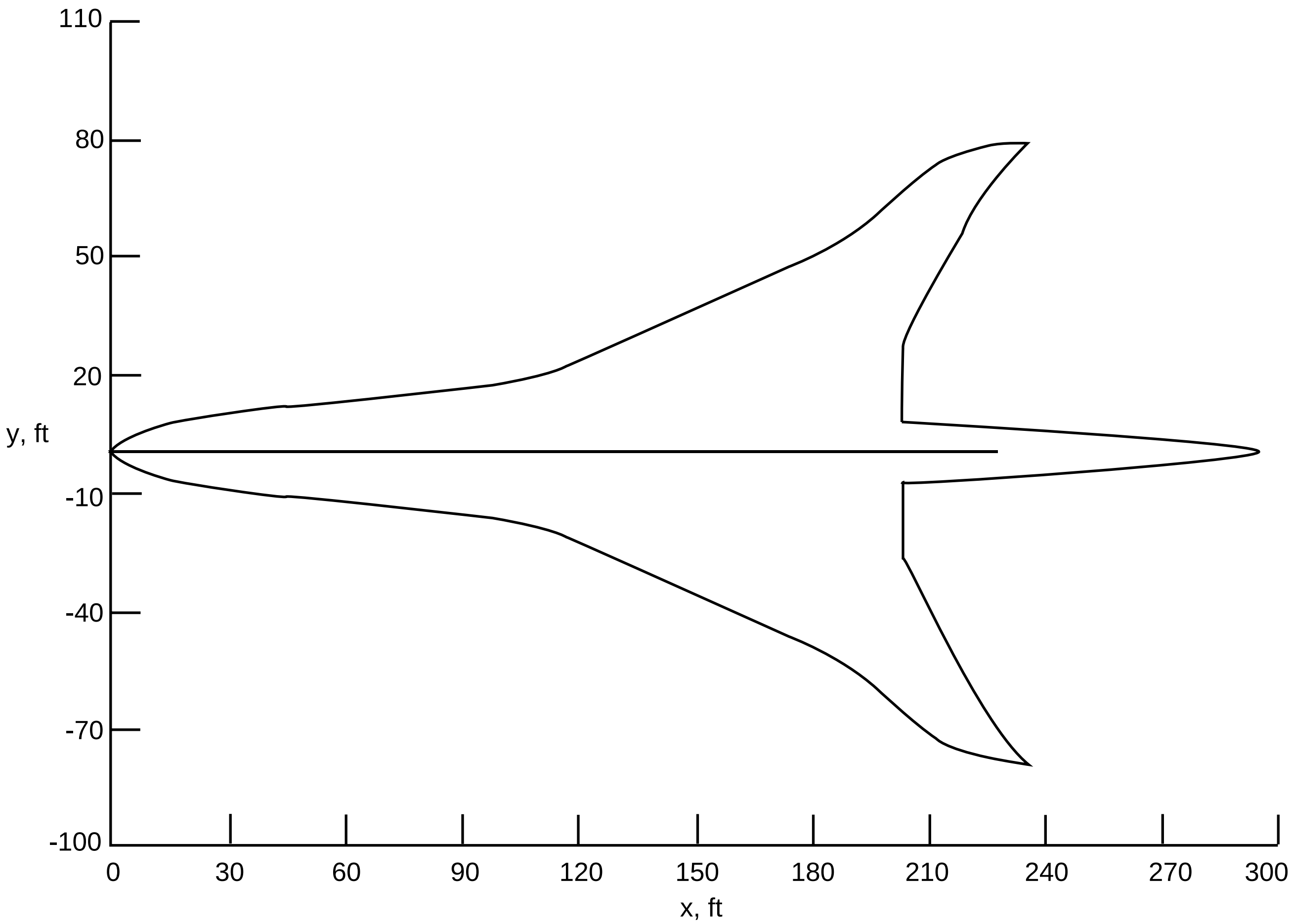

Figure 7. Planform of Mach 2.0 low-drag configuration.

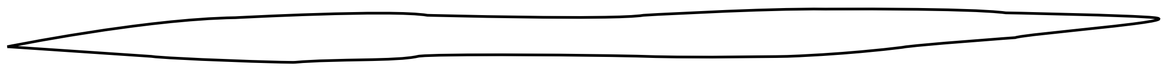

(a) Initial.

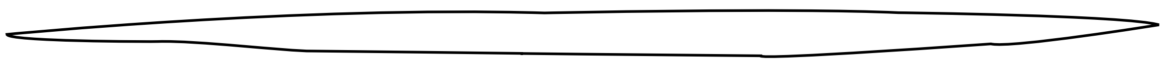

(b) Revised.

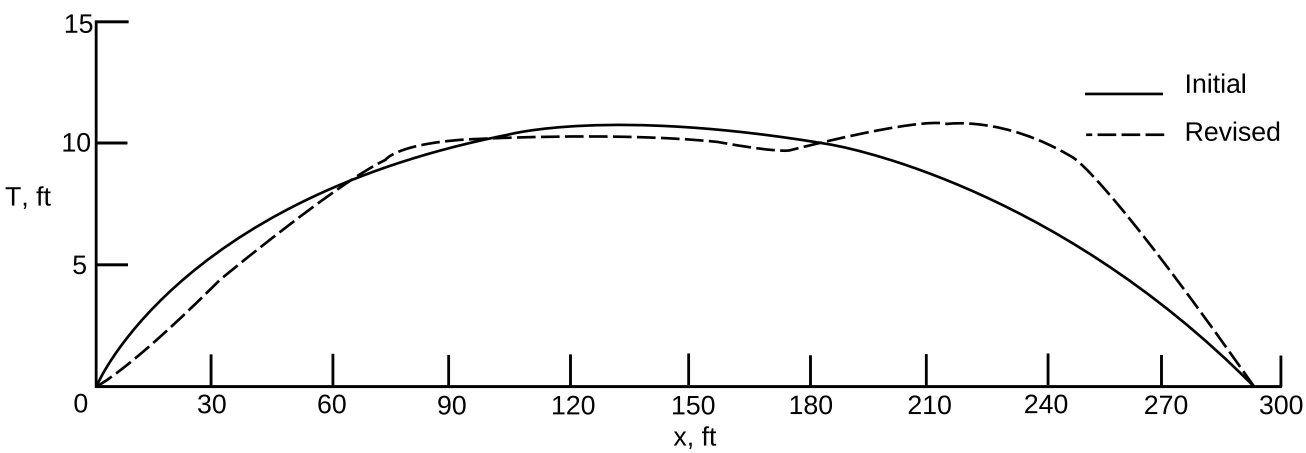

(c) Comparison of centerline thickness distributions.

Figure 8. Thickness distributions along centerline for Mach 2.0 low-drag configuration.

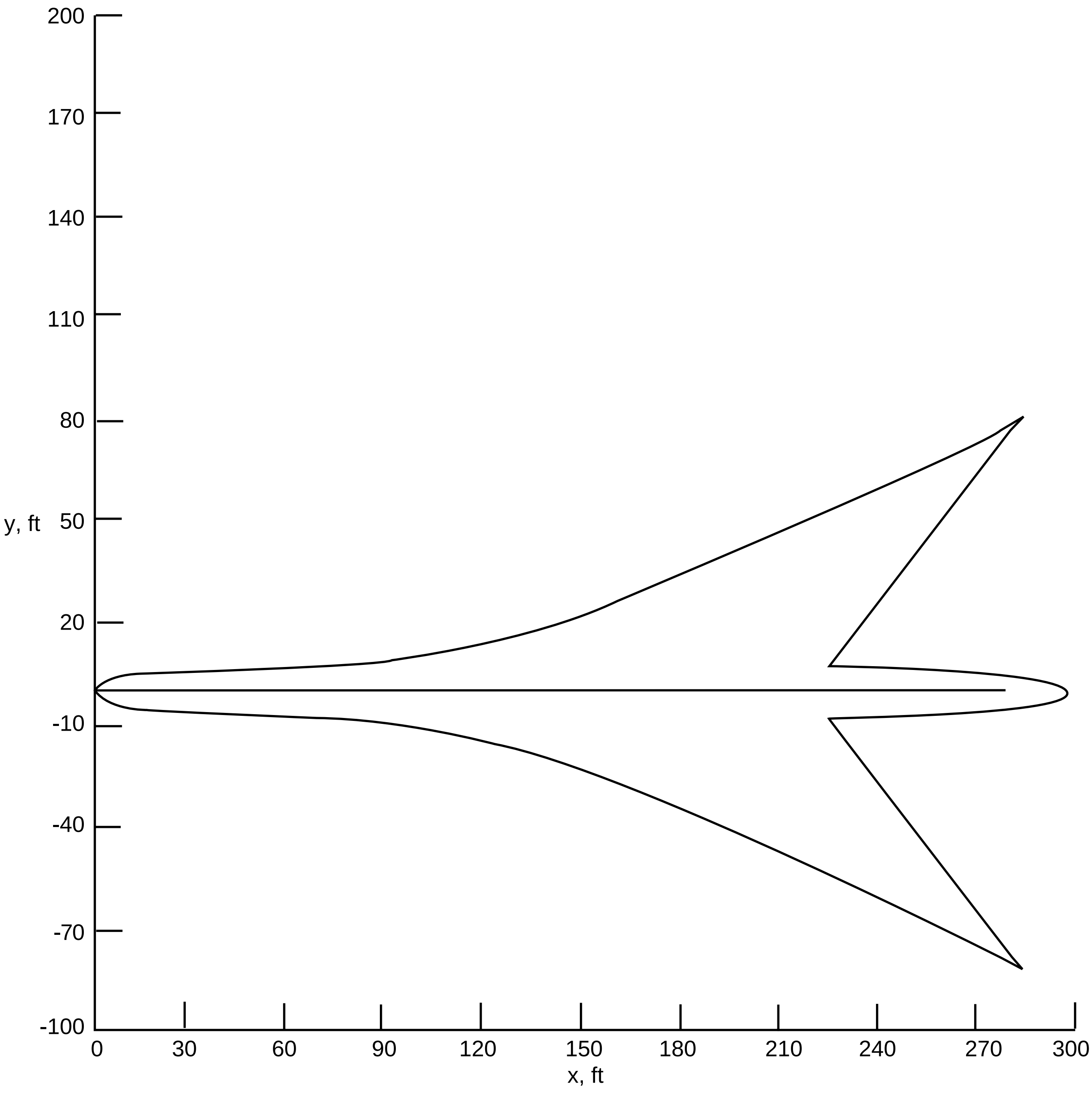

Figure 9. Planform of Mach 2.0 sonic-boom configuration.

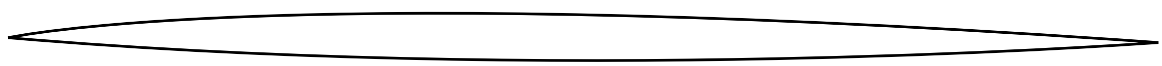

(a) Initial.

(b) Revised.

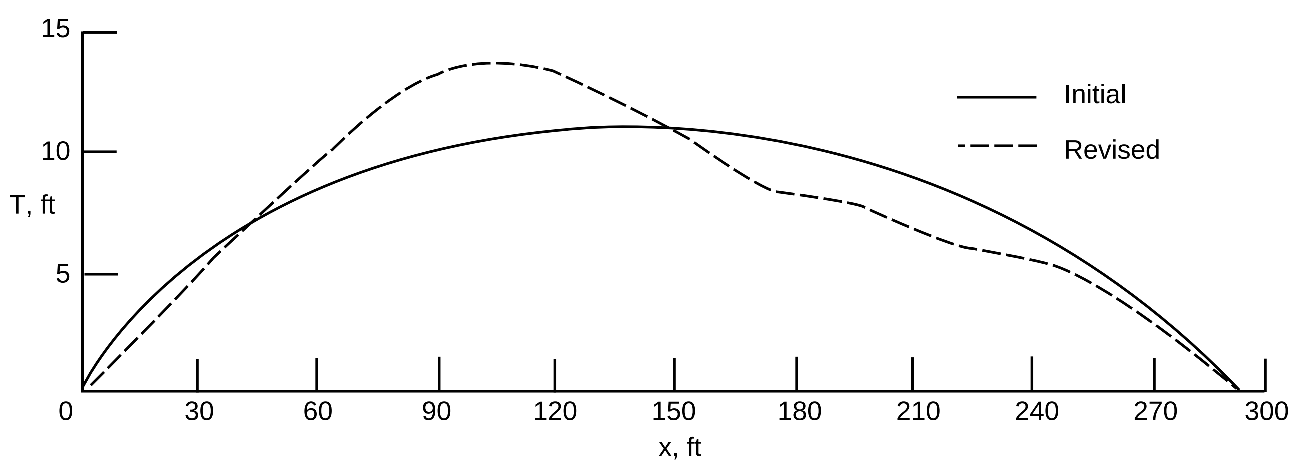

(c) Comparison of centerline thickness distributions.

Figure 10. Thickness distributions along centerline for Mach 2.0 sonic-boom configuration.

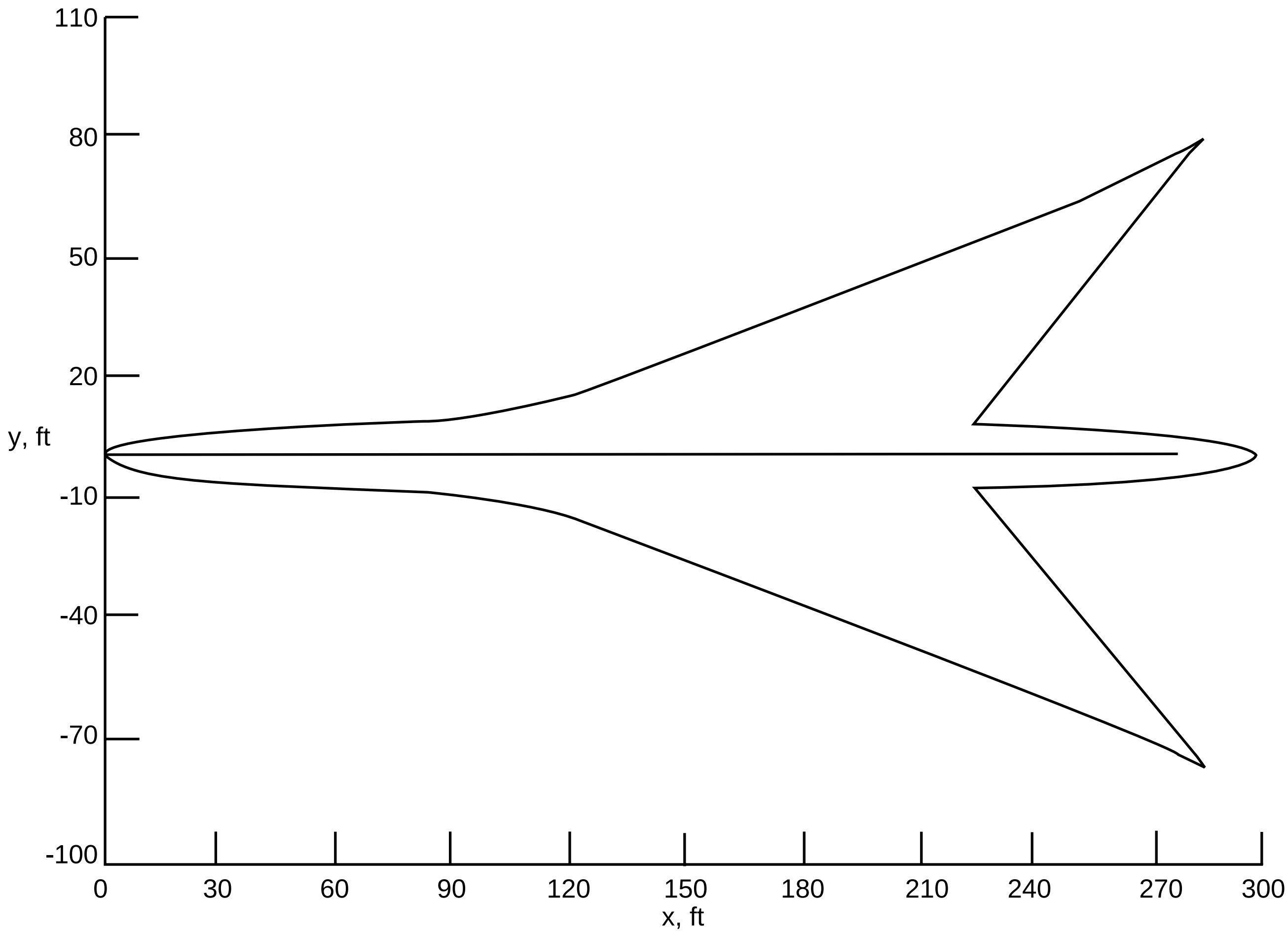

Figure 11. Planform of Mach 2.4 configuration.

(a) Initial.

(b) Revised.

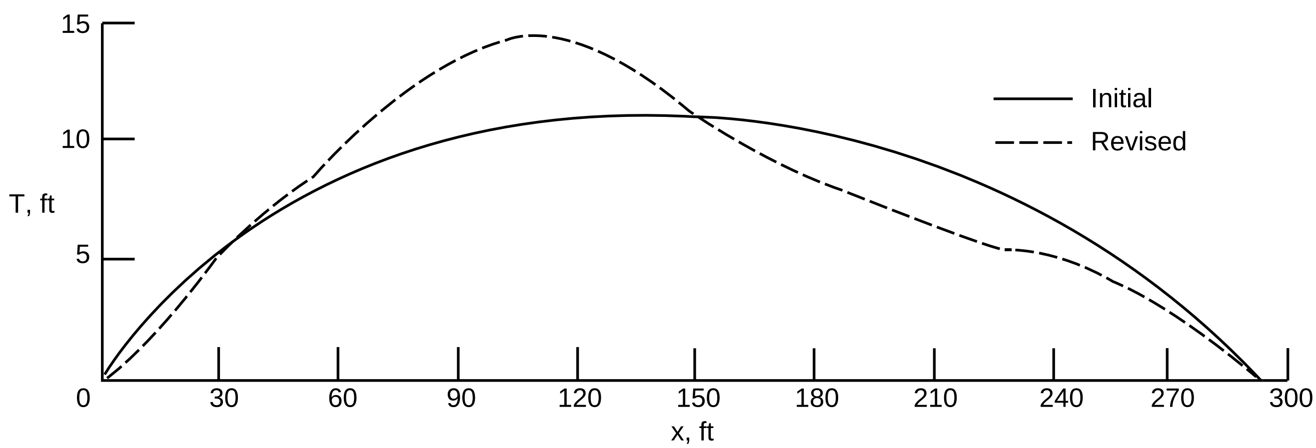

(c) Comparison of centerline thickness distributions.

Figure 12. Thickness distributions along centerline for Mach 2.4 configuration.